

Received June 3, 2021, accepted June 13, 2021, date of publication June 18, 2021, date of current version June 30, 2021.

Digital Object Identifier 10.1109/ACCESS.2021.3090369

# Recognition and Analysis of Unexpected Modes of Modular Multilevel Converter

XIAOFU FAN<sup>1</sup>, DONGYUAN QIU<sup>1</sup>, (Member, IEEE), BO ZHANG<sup>1</sup>, (Senior Member, IEEE),  
YANFENG CHEN<sup>1</sup>, (Member, IEEE), FAN XIE<sup>1</sup>, (Member, IEEE), AND CHANGHAI YUAN

School of Electric Power, South China University of Technology, Guangzhou 510641, China

Corresponding author: Dongyuan Qiu (epdyqiu@scut.edu.cn)

This work was supported in part by the National Key Research and Development Program of China under Grant 2018YFB0905803, and in part by the Natural Science Foundation Research Team Project of Guangdong Province under Grant 2017B030312001.

**ABSTRACT** The modular multilevel converter (MMC) with the clamp double submodule (CDSM) performs outstandingly on the handling of DC fault current. As CDSM is composed of multiple switching devices, different operating modes can be produced according to the combination of switching states. Among the effective operating modes, there are inevitably some unexpected modes, which may cause abnormal operation or even failure of the MMC. In order to improve the reliability of MMC, it is necessary to identify all the effective operating modes of CDSM and analyze their trigger conditions. In this article, a novel mode identification method for power converter with multiple switches is used. According to reasonable combination of switching states, the components of CDSM are connected in an orderly manner to obtain all effective operating modes. Based on the operating principle of CDSM, the unexpected modes are further recognized from the effective operating modes, so that the impact of the unexpected modes on the MMC can be obtained. Finally, the recognition and analysis results of the unexpected modes in CDSM is verified by Simulink and Plecs RT Box.

**INDEX TERMS** Modular multilevel converter (MMC), clamp double submodule (CDSM), operating mode, mode identification.

## I. INTRODUCTION

In 2003, the concept of modular multilevel converter (MMC) was firstly proposed [1]. Due to the distinguish advantages of high modularity [2], small harmonic content [3] and low converter losses [4], MMC has been widely used in high-voltage direct-current (HVDC) system. The topology of 3-phase MMC is shown in Fig. 1, which is composed of six arms. In each arm,  $n$  submodules (SM) and one inductor are connected in series. By controlling the output voltage of each SM, MMC can generate sinusoidal AC voltage [1].

As an important part of HVDC system, the reliability of MMC is crucial. Normally, MMC should have the ability to handle DC fault current and identify the component failures. There are three approaches to limit DC fault current: employing ac-side circuit breakers, employing dc-side circuit breakers and embedding submodules with DC fault handling capability. Since embedding submodules is more

effective than adding breakers, more attention is attracted on submodules [5].

Among the submodules used in MMC, the clamp double submodule (CDSM) has the ability of handling DC fault current because it can output negative capacitor voltage [6], [7]. In addition, compare with other types of submodule, CDSM can output more voltage levels and is more cost-effective, so it has become a popular SM in the MMC system [8], [9].

As shown in Fig.2, CDSM consists of five IGBTs with anti-parallel diodes, two clamp diodes and two capacitors. It is known that the on-off combination of switching devices will make the submodule operate in different modes [10]. Normal operating modes are those designed for certain functions, whereas unexpected modes or sneak circuit modes would not appear in normal cases but will occur in some specific conditions [11]. The appearance of unexpected modes will affect the output performance and bring potential risk on the operation of converters. By identifying all the unexpected modes in advance, further analysis on their trigger conditions as well as effects can be obtained. Therefore, the recognition of unexpected modes helps to ensure the performance

The associate editor coordinating the review of this manuscript and approving it for publication was Zhilei Yao<sup>1</sup>.

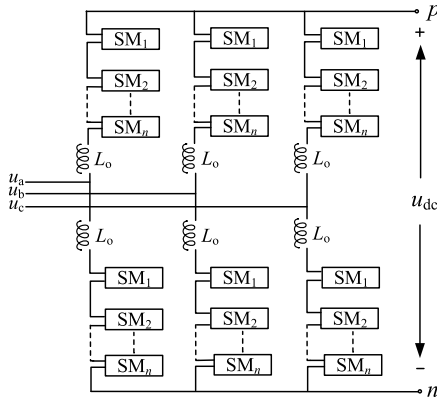


FIGURE 1. Topology of MMC.

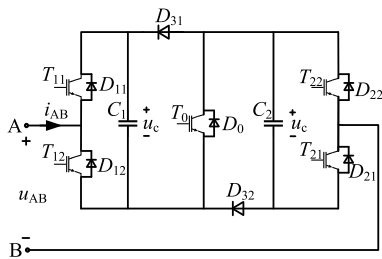


FIGURE 2. Topology of CDSM.

of converter as well as improve the reliability of operation. Generally, unexpected modes can be triggered by component failure [12], [13], control signal failure [11], variation of parameters [14] and so on. Not all unexpected modes are caused by component failure, so it is difficult to be detected. A complete view of detailed interrelationship between components and function is helpful to avoid the appearance of unexpected modes [15]. Furthermore, unexpected modes are controllable or avoidable if the trigger conditions of them are obtained [15].

Thus, to prevent the impact of unexpected modes of CDSM on MMC, a novel mode identification method is used in this article. The remainder of this article is organized in the following sections. Section II gives the introduction of mode identification principle. Section III introduces the mode recognition process of CDSM. After identifying all the effective operating modes of CDSM, unexpected modes are recognized and their trigger conditions as well as effects are further analyzed in section IV. During the recognition of unexpected modes on MMC, the novel mode identification method can obtain all the effective current paths which is effective and convenient. Then, simulation on Simulink/Matlab and experimental results on PLECS RT Box verify the impact of unexpected modes of CDSM in section V. In the end, the summary of this article is described in section VI

**II. MODE IDENTIFICATION PRINCIPLE**

Some methods have been invented to identify operating modes of power electronic converters including generalized connection matrix method, adjacency matrix method, and

mesh combination method [10], [14], [16], [17]. However, the above methods are not suitable for converters with large number of switching devices because the calculations and analysis complexity increase dramatically with the growing number of switching devices. To simplify the procedure of identifying modes and promise the completeness of result, a novel mode identification method is adopted in this article.

The basic process of this method is to obtain effective operating modes by connecting passive components with combinations of switching states. The main steps are as follow:

- 1) Generate component tree diagram based on the current paths of power electronic converter.
- 2) Classify switching states of switches in each level in the component tree diagram and then passive components in the same level are connected under the constrain conditions, so combinations of components in the same level can be obtained.
- 3) Connect combinations of components in each level successively, and effective operating modes can be generated.

This method takes topology of converter and operating principles into consideration when identifying effective operating modes. It is clear that the result of this method is intuitive and complete. Besides, the analysis process is also simple and fast.

**A. MODE RECOGNITION OF CDSM**

First, the component tree diagram can be obtained according to current paths. It starts with input port, grows with the current paths, and ends up with output port. Points in the component tree diagram represent components, and lines represent current paths. To simplify the analysis procedure, IGBT with anti-parallel diode can be considered as a bidirectional switching device  $S$  in the tree diagram, for example, both  $T_0$  and  $D_0$  are represented by  $S_0$ .

Since current can flow into the CDSM from both port A and port B, two component tree diagrams can be generated according to the current direction, which are shown in Fig. 3. In the component tree diagram, the input port is set as the first level component and the output port is set as the last level component. The rest of components in the tree diagram can be classified into different levels according to the sequence of current flow. Therefore, when  $i_{AB} > 0$ , the tree diagram is depicted in Fig.3(a); when  $i_{AB} < 0$ , the tree diagram is depicted in Fig.3(b).

The second step is to obtain combinations of components in each level. Components in the tree diagram can be sorted into switching devices and passive components. For switching devices, switching states can be divided into “ON” and “OFF” states. For example, there are two components ( $S_{12}$  and  $C_1$ ) in Level 3 of the component tree diagram in Fig.3(a). Since  $S_{12}$  has two switching states, connect passive components  $C_1$  to them will obtain two kinds of combinations of components in this level.

Thirdly, after obtaining combinations of components in each level, connect components in different levels orderly.

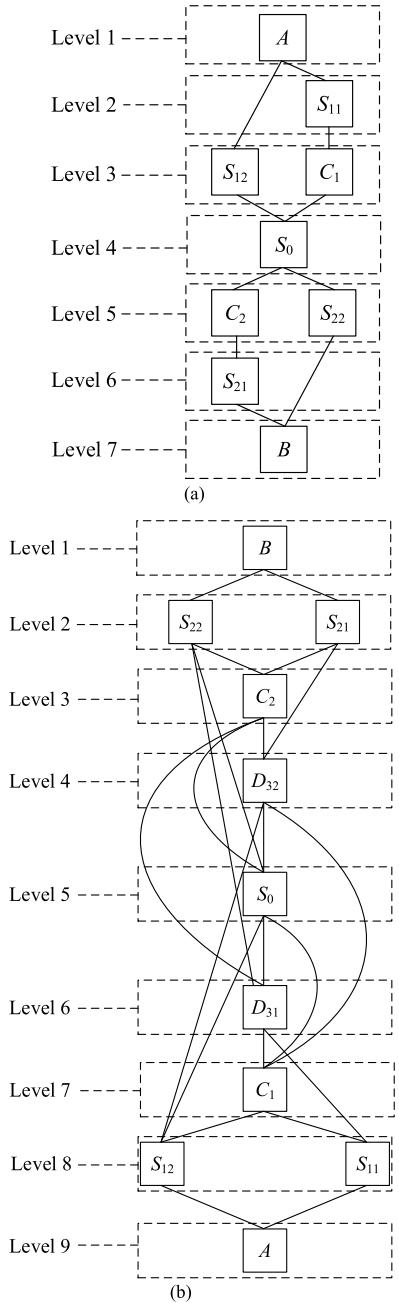


FIGURE 3. Tree diagrams of CDSM. (a) Current flows from port A to port B,  $i_{AB} > 0$ . (b) Current flows from port B to port A,  $i_{AB} < 0$ .

According to basic principles of circuit and operating principles of CDSM, some combinations of components are invalid, which should be abandoned. The constraint conditions are concluded as follow:

- 1) Diodes which connected in parallel operate in the same state. For example, when  $T_{21}$  and  $T_0$  switch on,  $D_{22}$  and  $D_{32}$  connected in parallel, in this case,  $D_{22}$  and  $D_{32}$  will be "ON" simultaneously if  $i_{AB} < 0$ .
- 2) When capacitors  $C_1$  and  $C_2$  are connected in parallel, both of them are "Connected" or "Bypass" at the same time. For example, when  $D_{31}$  and  $D_{32}$  are "ON",

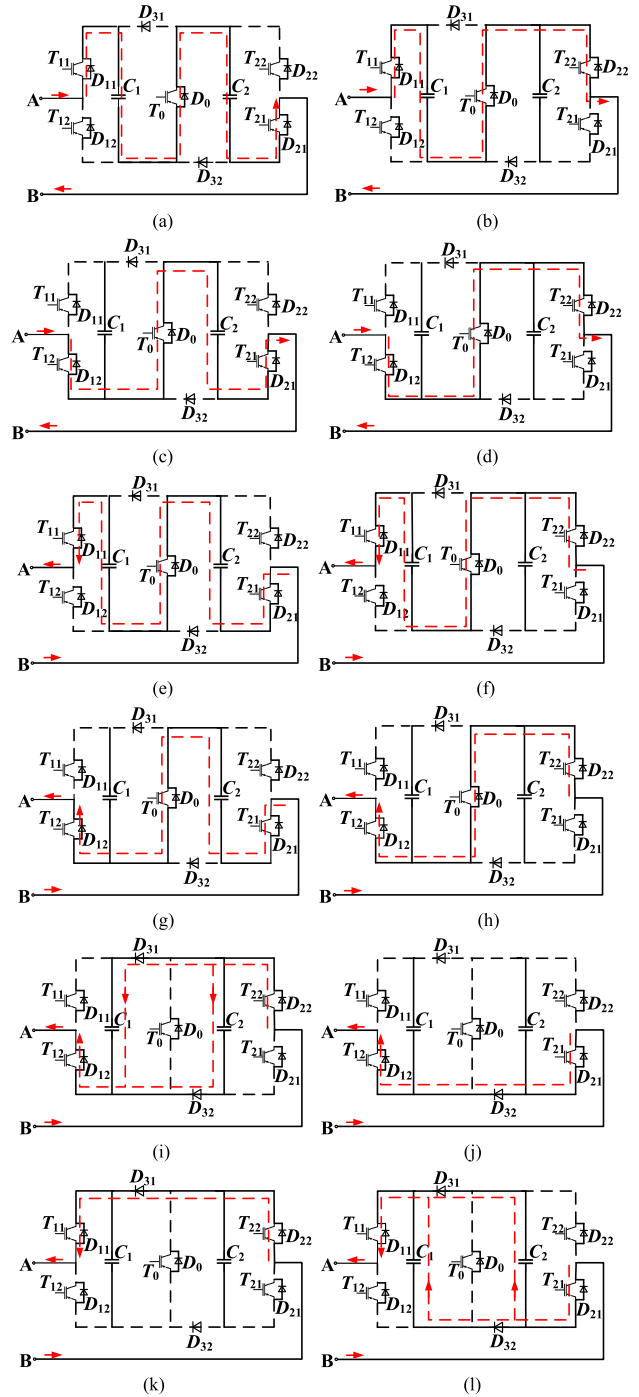


FIGURE 4. Effective modes of CDSM. (a) Mode 1. (b) Mode 2. (c) Mode 3. (d) Mode 4. (e) Mode 5. (f) Mode 6. (g) Mode 7. (h) Mode 8. (i) Mode 9. (j) Mode 10. (k) Mode 11. (l) Mode 12.

- $C_1$  and  $C_2$  are connected in parallel, they will be "Bypass" if  $S_0$  switches on.
- 3) Capacitors  $C_1$  and  $C_2$  cannot be short-circuit. For example, when  $S_0$  and  $D_{31}$  are "ON",  $C_1$  will be "Bypass"; when  $S_0$  and  $D_{32}$  are "ON",  $C_2$  will be "Bypass".

Take components in Level 2 and Level 3 of Fig.3(a) as an example. Level 2 contains a switching component  $S_{11}$  while

**TABLE 1. Normal operating modes and their corresponding switching states of CDSM.**

Mode Type	$T_{11}$	$T_{12}$	$T_{21}$	$T_{22}$	$T_0$	$u_{AB}$	$i_{AB}$
NM 1	1	0	0	1	1	$u_c$	$> 0$ or $< 0$
NM 2	1	0	1	0	1	$2u_c$	$> 0$ or $< 0$
NM 3	0	1	0	1	1	0	$> 0$ or $< 0$
NM 4	0	1	1	0	1	$u_c$	$> 0$ or $< 0$
NM 5	0	0	0	0	0	$2u_c$	$> 0$
NM 6	0	0	0	0	0	$-u_c$	$< 0$

Note: “1” represents for ON state, while “0” represents for OFF state. “NM” represents for normal operating mode.

**TABLE 2. Operating modes of CDSM and their current paths.**

Mode No.	Type	Current path
Mode 1	NM2/5	$A-D_{11}-C_1-D_0-C_2-D_{21}-B$
Mode 2	NM 1	$A-D_{11}-C_1-D_0-T_{22}-B$
Mode 3	NM 4	$A-T_{12}-D_0-C_2-D_{21}-B$
Mode 4	NM 3	$A-T_{12}-D_0-T_{22}-B$
Mode 5	NM 2	$B-T_{21}-C_2-T_0-C_1-T_{11}-A$
Mode 6	NM 1	$B-D_{22}-T_0-C_1-T_{11}-A$
Mode 7	NM 4	$B-T_{21}-C_2-T_0-D_{12}-A$
Mode 8	NM 3	$B-D_{22}-T_0-D_{12}-A$
Mode 9	NM 6	$B-D_{22}-D_{31}-C_1-D_{12}-A, B-D_{22}-C_2-D_{32}-D_{12}-A$
Mode 10	UM1	$B-T_{21}-D_{32}-D_{12}-A$
Mode 11	UM2	$B-D_{22}-D_{31}-T_{11}-A$
Mode 12	UM3	$B-T_{21}-D_{32}-C_1-T_{11}-A, B-T_{21}-C_2-D_{31}-T_{11}-A$

Note: “UM” represents for unexpected mode.

**TABLE 3. Comparison results between normal operating modes and unexpected modes ( $i_{AB} < 0$ ).**

Mode No.	Mode Type	Common Components	Different Components
7	NM		$C_2, T_0$
10	UM	$T_{21}, D_{12}$	$D_{32}$
6	NM		$C_1, T_0$
11	UM	$D_{22}, T_{11}$	$D_{31}$
5	NM	$T_{11}, T_{21}$	$T_0$
12	UM	$C_1, C_2$	$D_{31}, D_{32}$

Level 3 contains a switching component  $S_{12}$  and a passive component  $C_1$ . Under the constrain conditions, the effective combinations of components in these two levels are:

- $S_{11}$  is “ON”,  $S_{12}$  is “ON”,  $C_1$  is “Bypass”;
- $S_{11}$  is “ON”,  $S_{12}$  is “OFF”,  $C_1$  is “Connected”;
- $S_{11}$  is “ON”,  $S_{12}$  is “OFF”,  $C_1$  is “Bypass”;
- $S_{11}$  is “OFF”,  $S_{12}$  is “ON”,  $C_1$  is “Connected”;
- $S_{11}$  is “OFF”,  $S_{12}$  is “ON”,  $C_1$  is “Bypass”.

**TABLE 4. Performance of different operating modes.**

$T_0$ Fails	Mode No.	$u_{AB}$	States of $C_1, C_2$
Before	5	$2u_c$	discharge
After	12	$u_c$	discharge
Before	6	$u_c$	$C_1$ discharge
After	11	0	/
Before	7	$u_c$	$C_2$ discharge
After	10	0	/
Before	8	0	/
After	9	$u_c$	$C_1, C_2$ charge

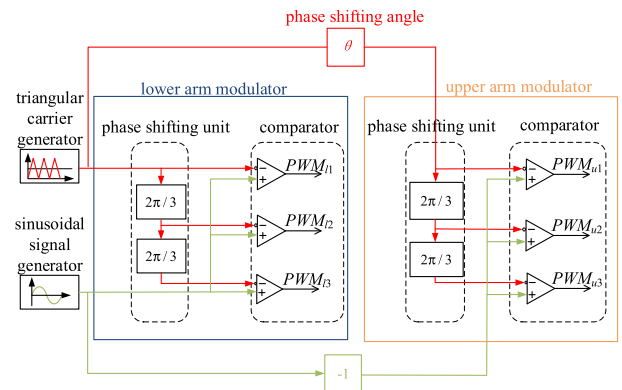


**FIGURE 5. Diagram of the PSC-PWM applied to MMC.**

**TABLE 5. Simulation parameters of CDSM.**

Item	Value
number of submodular in each arm $N$	3
capacitor $C_1, C_2$ ( $\mu\text{F}$ )	200
DC voltage $V_{dc}$ (V)	200
triangular carrier frequency $f_c$ (kHz)	1.25
reference frequency $f_r$ (Hz)	50
inductance of bridge arm $L_i$ (mH)	1
resistance bridge arm $R_i$ ( $\Omega$ )	2
resistance load $R_z$ ( $\Omega$ )	500
inductance load $L_z$ (mH)	1
modulation ratio	0.87

Therefore, according to the tree diagrams of CDSM, effective operating modes can be obtained by connecting switching states and passive components under constraint conditions. In Fig. 3(a), when  $S_{11}, S_0$ , and  $S_{21}$  are “ON”, the corresponding current path is  $A-S_{11}-C_1-S_0-C_2-S_{21}-B$  and Mode 1 is generated (Fig. 4(a)). Similarly, other modes in Fig. 3(a) can be obtained, which are

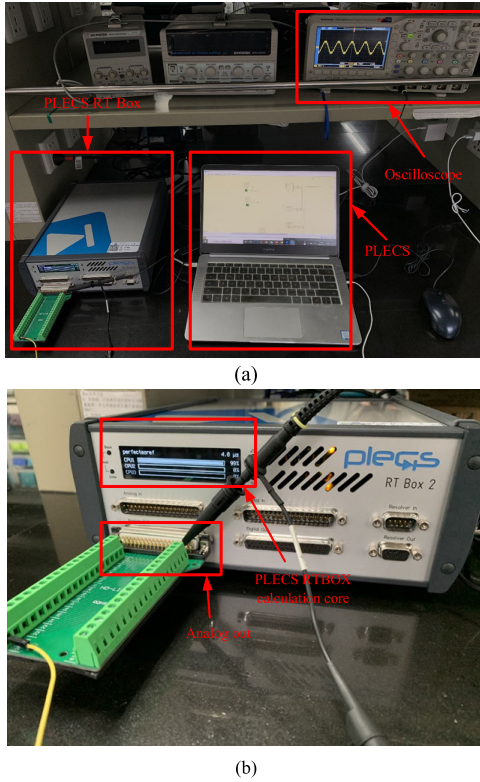


FIGURE 6. Setup of plects RT box.

- (1) When  $S_{11}$ ,  $S_0$ , and  $S_{22}$  are “ON”, the corresponding current path is A- $S_{11}$ - $C_1$ - $S_0$ - $S_{22}$ -B, and Mode 2 is generated (Fig. 4(b));
- (2) When  $S_{12}$ ,  $S_0$ , and  $S_{21}$  are “ON”, the corresponding current path is A- $S_{12}$ - $S_0$ - $C_2$ - $S_{21}$ -B, and Mode 3 is generated (Fig. 4(c));
- (3) When  $S_{12}$ ,  $S_0$ , and  $S_{22}$  are “ON”, the corresponding current path is A- $S_{12}$ - $S_0$ - $S_{22}$ -B, and Mode 4 is generated (Fig. 4(d)).

The operating modes according to Fig. 3(b) can be obtained by the same method. As a result, there are 8 operating modes when  $i_{AB} < 0$ , which are shown in Fig. 4(e) - Fig. 4(l), respectively.

### III. MODE IDENTIFICATION RESULT OF CDSM

From Fig.2, CDSM can be regarded as two series-connected half-bridge converters. MMC outputs the desired voltage when  $S_0$  is “ON” in CDSM, and blocks the fault current by turning off all IGBTs in CDSM. Thus, all normal operating modes of CDSM are summarized in Table. 1.

Compare the effective modes in Fig.4 with Table. 1, those modes with the same current paths in Table. 1 are normal operating modes, and the rest modes in Fig.4 are unexpected modes. Table. 2 classifies the types of all effective operating modes of CDSM, it is found that Mode 1 to Mode 9 are the normal modes and Mode 10 to Mode 12 are the unexpected ones.

Based on the current paths of unexpected modes in Table. 2, the triggered conditions of unexpected modes can be

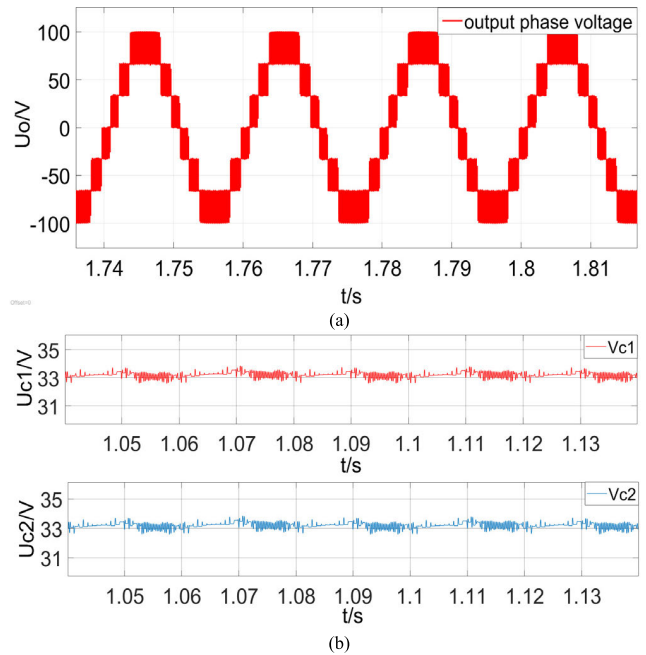


FIGURE 7. Simulation results when CDSM-MMC operates in normal operating modes. (a) Output voltage. (b) Capacitor voltage.

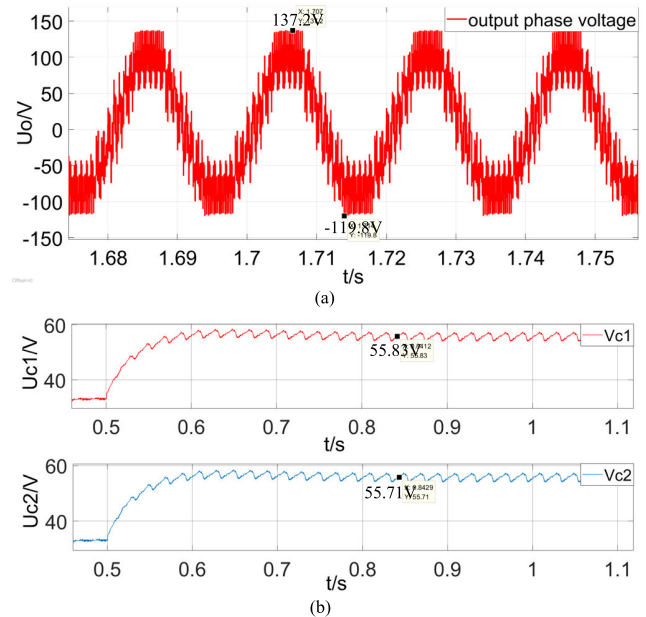


FIGURE 8. Simulation results when CDSM-MMC operates in unexpected modes. (a) Output voltage. (b) Capacitor voltage.

deduced. When  $T_{12}$  and  $T_{21}$  switch on,  $T_{11}$  and  $T_{22}$  switch off, current flows through  $D_{32}$  in Mode 10 rather than  $C_2$  and  $T_0$  in Mode 7. When  $T_{11}$  and  $T_{22}$  switch on,  $T_{12}$  and  $T_{21}$  switch off, current flows through  $D_{31}$  in Mode 11 rather than  $C_1$  and  $T_0$  in Mode 6. When  $T_{11}$  and  $T_{21}$  switch on,  $T_{12}$  and  $T_{22}$  switch off, current flows through  $D_{31}$  and  $D_{32}$  in Mode 12 rather than  $T_0$  in Mode 5. Besides, all the above unexpected modes occur only when  $i_{AB} < 0$ . The comparison results of current paths between normal operating modes and unexpected modes are concluded in Table. 3.

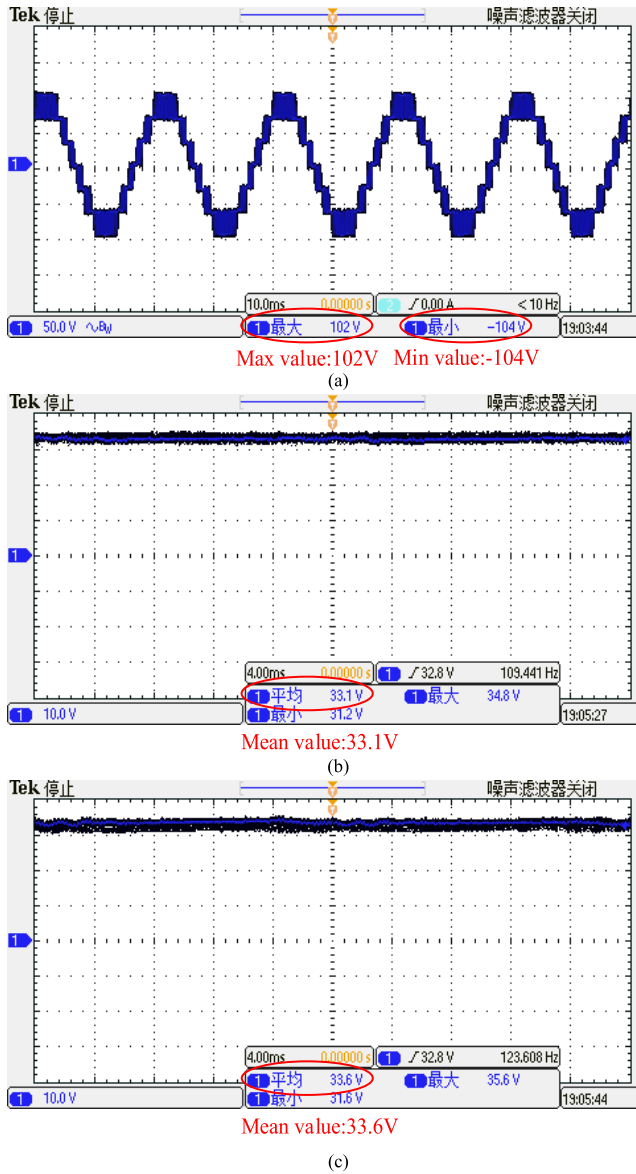


FIGURE 9. Experiment results when CDSM-MMC operates in normal operating modes. (a) Output voltage. (b) Capacitor voltage  $u_{c1}$ . (c) Capacitor voltage  $u_{c2}$ .

As shown in Table 3, when  $C_2$  has open-circuit failure, unexpected Mode 10 will appear; when  $C_1$  has open-circuit failure, unexpected Mode 11 will appear. When  $T_0$  has open-circuit failure or drive failure, unexpected Mode 10, Mode 11, and Mode 12 will appear when current flows from port B to port A. CDSM will operate in different operating modes when  $T_0$  fails, and the output voltage of submodule as well as states of capacitors may change. Once  $T_0$  fails, apart from the trigger of unexpected modes (Mode 10 to Mode 12), normal operating mode will also be affected. Since current flows through  $T_0$  in Mode 8, CDSM will not operate in Mode 8 but will operate in Mode 9 when  $T_0$  fails. The output voltage as well as states of capacitors in CDSM of these modes could be obtained in Fig.4. Table 4 concludes the different performance of CDSM before and after  $T_0$  fails. It is shown

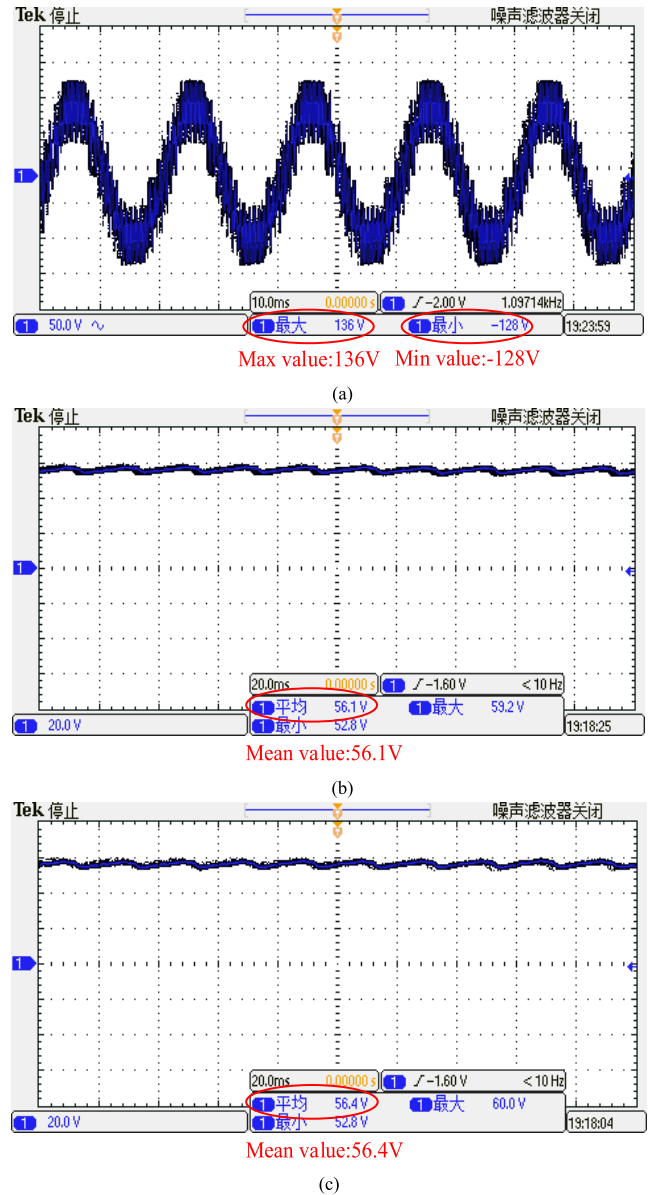


FIGURE 10. Experiment results when CDSM-MMC operates in unexpected modes. (a) Output voltage. (b) Capacitor voltage  $u_{c1}$ . (c) Capacitor voltage  $u_{c2}$ .

that the output voltage of submodule  $u_{AB}$  decreases when unexpected modes occur, which will lead the output voltage of CDSM-MMC to be distorted. Besides, the number of discharged modes for capacitors decreases, thus the capacitor voltages of CDSM will increase after the unexpected modes are triggered.

#### IV. VERIFICATIONS

In this section, Simulink/Matlab is used to verify the effects of unexpected modes of CDSM, and Plects RT Box [18] is used in experimental verification. The RT Box is a technical solution of Plexim GmbH in which the simulation models are realized in the Plects simulation environment. Then, the simulation models are transformed into real-time models with minimal changes [19]. As the results are

communicated by Ethernet, the real-time results can be captured [20].

The phase-shifted carrier modulation method (PSC) is applied here [21], [22], which is shown in Fig.5. In this figure, the phase shifting angle  $\theta$  is related to the harmonic content. In order to output the least harmonic content,  $\theta$  equals to 0 when the number of submodules in one bridge arm is odd;  $\theta$  equals to  $\pi/N$  when the number of submodules in one bridge arm is even [23]. Assuming that MMC has three CDSMs ( $N = 3$ ) in each bridge arm, in this case,  $\theta = 0$ . The simulation parameters of MMC are listed in Table. 5. In the Table. 5, there is a virtual resistor in each arm to represent the loss of MMC [24]. The experimental setup of Plecs RT Box is shown in Fig.6.

When MMC operates normally, simulation results are shown in Fig.7. If  $T_0$  in SM1 fails, unexpected modes will be triggered, the corresponding simulation results are shown in Fig.8. The experiment results of the above two situations are shown in Fig.9 and Fig.10, respectively.

When CDSM-MMC operates in normal operating modes, the output voltage has 7 levels and the capacitor voltages are about 33V. When SM1 in CDSM-MMC operates in unexpected modes, the output voltage in MMC is distorted. The capacitor voltages of the failed SM1 will increase to about 56.1V and 56.4V, respectively. In conclusion, the simulation and experiment results are match with the analysis.

## V. CONCLUSION

This article describes an unexpected mode identification method and applies it to CDSM-MMC. This method utilizes the ordered connection of components in the converter to obtain all effective operating modes, and some unexpected modes of CDSM are detected. After that, the trigger conditions and effects of unexpected modes in CDSM is further analyzed. Finally, Simulink/Matlab and Plecs RT Box are used to verify the analysis results of unexpected modes on output performance of CDSM-MMC. As the results show, when unexpected modes are triggered, the output voltage of CDSM-MMC will be distorted, whose max and min values will change from about  $\pm 100V$  to  $+136V$  and  $-128V$ , respectively. The capacitor voltages of the failed SM1 will increase from nearly 33V to about 56.1V and 56.4V, respectively.

The mode identification method for power electronic converters has the following advantages: 1) it uses the constraint conditions to screen some invalid modes during the process of component connection, which can reduce the redundant modes; 2) all effective operating modes are obtained directly by connecting components orderly, so the results are concise and clear. Besides, this mode identification method can be applied to other power electronic converters which can help to find unexpected modes, analyze their triggered conditions and the effects of unexpected modes on the converter systems.

## REFERENCES

- [1] A. Lesnicar and R. Marquardt, "An innovative modular multilevel converter topology suitable for a wide power range," in *Proc. IEEE Bologna Power Tech Conf.*, Jun. 2003, p. 6.
- [2] R. Marquardt, "Modular multilevel converter: An universal concept for HVDC-networks and extended DC-bus-applications," in *Proc. Int. Power Electron. Conf. (ECCE) ASIA*, Jun. 2010, pp. 502–507.
- [3] E. Kontos, G. Tsolaridis, R. Teodorescu, and P. Bauer, "High order voltage and current harmonic mitigation using the modular multilevel converter STATCOM," *IEEE Access*, vol. 5, pp. 16684–16692, 2017.
- [4] P. Ladoux, P. Marino, G. Raimondo, and N. Serbia, "Comparison of high voltage modular AC/DC converters," in *Proc. Int. Symp. Power Electron. Power Electron., Electr. Drives, Autom. Motion*, Jun. 2012, pp. 843–848.
- [5] Y. Xue and Z. Xu, "On the bipolar MMC-HVDC topology suitable for bulk power overhead line transmission: Configuration, control, and DC fault analysis," *IEEE Trans. Power Del.*, vol. 29, no. 6, pp. 2420–2429, Dec. 2014.
- [6] S. Debnath, J. Qin, B. Bahrani, M. Saedifard, and P. Barbosa, "Operation, control, and applications of the modular multilevel converter: A review," *IEEE Trans. Power Electron.*, vol. 30, no. 1, pp. 37–53, Jan. 2015.
- [7] R. Marquardt, "Modular multilevel converter topologies with DC-short circuit current limitation," in *Proc. 8th Int. Conf. Power Electron. (ECCE) Asia*, May 2011, pp. 1425–1431.
- [8] T. Modeer, H.-P. Nee, and S. Norrga, "Loss comparison of different sub-module implementations for modular multilevel converters in HVDC applications," *EPE J.*, vol. 22, no. 3, pp. 32–38, Sep. 2012.
- [9] G. Tang, Z. Xu, and Y. Zhou, "Impacts of three MMC-HVDC configurations on AC system stability under DC line faults," *IEEE Trans. Power Syst.*, vol. 29, no. 6, pp. 3030–3040, Nov. 2014.
- [10] Y. Ma and K. M. Smedley, "Switching flow-graph nonlinear modeling method for multistate-switching converters," *IEEE Trans. Power Electron.*, vol. 12, no. 5, pp. 854–861, Sep. 1997.
- [11] B. Zhang, "Sneak circuits in power converters: Concept, principle and application," *CPSS Trans. Power Electron. Appl.*, vol. 2, no. 1, pp. 68–75, Apr. 2017.
- [12] B. Li, S. Shi, B. Wang, G. Wang, W. Wang, and D. Xu, "Fault diagnosis and tolerant control of single IGBT open-circuit failure in modular multilevel converters," *IEEE Trans. Power Electron.*, vol. 31, no. 4, pp. 3165–3176, Apr. 2016.
- [13] Y. Yang, A. Sangwongwanich, and F. Blaabjerg, "Design for reliability of power electronics for grid-connected photovoltaic systems," *CPSS Trans. Power Electron. Appl.*, vol. 1, no. 1, pp. 92–103, Dec. 2016.
- [14] J. Li, D. Qiu, and B. Zhang, "Sneak circuit analysis for n-stage resonant switched capacitor converters based on graph theory," in *Proc. IECON 33rd Annu. Conf. IEEE Ind. Electron. Soc.*, Nov. 2007, pp. 1581–1585.
- [15] D. S. Savakoor, J. B. Bowles, and R. D. Bonnell, "Combining sneak circuit analysis and failure modes and effects analysis," in *Proc. RAMS*, Atlanta, GA, USA, Jan. 1993, pp. 199–205.
- [16] L. L. Qu, B. Zhang, D. Y. Qiu, and W. J. Tu, "Sneak circuit analysis method based on generalized connection matrix for power converters," in *Proc. Int. Conf. Electr. Mach. Syst.*, Wuhan, China, Oct. 2008, pp. 1587–1590.
- [17] R. R. Soman, E. M. Davidson, S. D. J. McArthur, J. E. Fletcher, and T. Ericson, "Model-based methodology using modified sneak circuit analysis for power electronic converter fault diagnosis," *IET Power Electron.*, vol. 5, no. 6, pp. 813–826, Jul. 2012.
- [18] X. Li, Z. Liang, M. Kleiner, and Z.-L. Lu, "RTbox: A device for highly accurate response time measurements," *Behav. Res. Methods*, vol. 42, no. 1, pp. 212–225, Feb. 2010.
- [19] A. Peric, H. Paukovic, M. Miletic, and V. Sunde, "Development of voltage source converter using HiL simulation system," in *Proc. 42nd Int. Conv. Inf. Commun. Technol., Electron. Microelectron. (MIPRO)*, May 2019, pp. 168–173.
- [20] A. Srinivasan, J. Moirangthem, S. K. Panda, and K. R. Krishnanand, "Hardware-in-loop control of a standalone microgrid," in *Proc. IEEE Int. Conf. Sustain. Energy Technol. (ICSET)*, Feb. 2019, pp. 365–370.
- [21] B. Li, Z. Xu, J. Ding, and D. Xu, "Fault-tolerant control of medium-voltage modular multilevel converters with minimum performance degradation under submodule failures," *IEEE Access*, vol. 6, pp. 11772–11781, 2018.
- [22] K. Ilves, L. Harnefors, S. Norrga, and H.-P. Nee, "Analysis and operation of modular multilevel converters with phase-shifted carrier PWM," *IEEE Trans. Power Electron.*, vol. 30, no. 1, pp. 268–283, Jan. 2015.
- [23] B. B. Li, "Research on modular multilevel converter and its control schemes," Ph.D. dissertation, Dept. Electron. Eng., Harbin Inst. Tech., Harbin, China, 2017.
- [24] F. Deng, Y. Lu, C. Liu, Q. Heng, Q. Yu, and J. Zhao, "Overview on submodule topologies, modeling, modulation, control schemes, fault diagnosis, and tolerant control strategies of modular multilevel converters," *Chin. J. Electr. Eng.*, vol. 6, no. 1, pp. 1–21, Mar. 2020.



**XIAOFU FAN** was born in Guangdong, China, in 1996. She received the B.S. degree in electrical engineering and automation from the Shanghai University of Electric Power, Shanghai, China, in 2018, and the M.Sc. degree from the South China University of Technology, Guangzhou, China, in 2021.

Her main research interests include mode identification and reliability analysis for power electronics.



**DONGYUAN QIU** (Member, IEEE) was born in Guangdong, China, in 1972. She received the B.Sc. and M.Sc. degrees from the South China University of Technology, Guangzhou, China, in 1994 and 1997, respectively, and the Ph.D. degree from the City University of Hong Kong, Hong Kong, in 2002.

She is currently a Professor with the School of Electric Power, South China University of Technology. She has authored or coauthored four books and over 200 articles, and holds more than 100 patents. Her main research interests include wireless power transfer, fault diagnosis, and sneak circuit analysis of power electronic systems. She is an Associate Editor of the IEEE TRANSACTIONS ON POWER ELECTRONICS.



**BO ZHANG** (Senior Member, IEEE) was born in Shanghai, China, in 1962. He received the B.Sc. degree in electrical engineering from Zhejiang University, Hangzhou, China, in 1982, the M.Sc. degree in power electronics from Southwest Jiaotong University, Chengdu, China, in 1988, and the Ph.D. degree in power electronics from the Nanjing University of Aeronautics and Astronautics, Nanjing, China, in 1994.

He is currently a Professor with the School of Electric Power, South China University of Technology, Guangzhou, China. He has authored or coauthored nine books and over 500 technical articles, and holds over 100 patents. His current research interests include nonlinear analysis, modeling and control of power electronic converters, and wireless power transfer applications.



**YANFENG CHEN** (Member, IEEE) received the M.Sc. degree in power electronics technology from Wuhan University, Wuhan, China, in 1995, and the Ph.D. degree in circuits and systems from the South China University of Technology, Guangzhou, China, in 2000.

From November 2005 to December 2006, she was a Research Associate with the Department of Electronic and Information Engineering, The Hong Kong Polytechnic University, Hong Kong. She is currently a Professor with the School of Electric Power, South China University of Technology. She has authored or coauthored three books, and more than 50 articles and 50 patents. Her main research interests include modeling and analysis of nonlinear systems and power electronics.



**FAN XIE** (Member, IEEE) received the B.S. and M.S. degrees in physics and physical electronics from the School of Physics and Electron Engineering, Guangzhou University, Guangzhou, China, in 2008 and 2011, respectively, and the Ph.D. degree in power electronics from the South China University of Technology, Guangzhou, in 2014.

In 2014, he joined the School of Electric Power, South China University of Technology, where he has been an Associate Professor, since 2018. His research interests include nonlinear dynamics of power electronic circuits, and control of power supplies and ac drives.



**CHANGHAI YUAN** was born in China, in 1995. He received the B.S. degree in electrical engineering from Nanchang University, Nanchang, China, in 2018, and the M.Sc. degree from the South China University of Technology, Guangzhou, China, in 2021.

He participated in the National Key Research and Development Program of China. His current research interests include analysis of power converters in power electronic systems and its applications in renewable energy.

...